

doi:10.15199/48.2020.11.30

Intelligent distance measuring module using ultrasonic piezoelectric ceramic transducers

Abstract. The paper deals with a complete design of a distance measuring module using commercially available piezoelectric ceramic transducers. Uniqueness of this module is harmonic signal generation, automatic frequency and amplitude control, automatic gain control and automatic detection level control. To reduce module measurement inaccuracy, a polynomial correction algorithm is implemented. Functional verification is performed here by a detailed analysis of relative error development.

Streszczenie. W artykule przedstawiono projekt urządzenia do pomiaru odległości wykorzystującego dostępne na rynku czujniki piezoelektryczne. Nowością jest inteligentne sterowanie pomiarem. Przedstawiono badania modelu i określono błąd pomiaru. (Inteligentny pomiar odległości z wykorzystaniem ultradźwiękowych czujników piezoelektrycznych)

Keywords: ultrasound, piezoelectric ceramic transducer, distance measurement, relative error.

Słowa kluczowe: pomiar odległości (dystansu), czujniki piezoelektryczne.

Introduction

Ultrasonic technologies are used in various areas of human activities. These areas include, for example, healthcare, mechanical engineering, automotive industry, security technologies and electro technical industry. Significant use is in the area of sensor technologies. The most common ultrasonic application is a distance measurement [1, 2, 3, 4]. This is used during obstacles detection and distance measurement from it in car parking assist systems and in unmanned means to collision avoidance of obstacles as local closed area navigation [5].

This paper is devoted to the description of the module that allows to measure distance and can be implemented in these applications. The basic principle of a distance measurement is to determine the time when the reflected acoustic wave returns from an obstacle. The acoustic wave is represented by a group of several periods of the transmitted signal. Knowing the acoustic wave velocity in the air and the measured time, the obstacle distance is determined [6].

This module uses a piezoelectric ceramic transducer as an acoustic wave transmitter and receiver that is easily available at the market and is economically undemanding. The disadvantage of the piezoelectric ceramic transducers is the dependence of their resonant frequency on a temperature [7]. The module has designed signal generator with the possibility to change the frequency and thus respects the variance in the resonant frequency of the transducer. It also works with a change of the signal amplitude for the range control. It creates a harmonic signal for later application of intra-pulse modulations and to ensure more accurate distance measurement. It also provides a choice of the number of periods of the transmitted signal to effectively excite the transducer. The module receiver is equipped with a threshold control for efficient extraction of a useful received signal from a noise and digitally controlled signal amplification. The range is also possible to influence by that. These operations are performed by a single-chip microprocessor. The above mentioned attributes are not implemented in ultrasonic distance measurement systems or are not described in the technical documentation [8, 9].

The module design

The designed and manufactured module consists of Transmitter block that generates an acoustic signal to the space. Another block is Receiver that performs analogue preprocessing of the acoustic signal reflected from the obstacle. Function control block provides setting of required

module parameters and consists of four micro buttons. The LCD block displays the obstacle distance value and module setting parameters. A four-line alphanumeric display has been selected, where it is possible to depict twenty characters. This display unit was equipped with a converter for serial communication via I2C bus [10]. The Power supply block provides electric energy to all module subsystems. The linear stabilizers 78M05 and 78M12 [11, 12] were used for providing the necessary supply voltages. A single-chip microprocessor provides reception of instructions from the module setup block, the method of transmitting the signal, processing the received signal, calculating the distance, performing correction, and transmitting the necessary information to the display unit. The ATmega328 microcontroller on the Arduino Nano platform [13] was chosen for this application. The block diagram of the complete module is shown in Fig. 1.

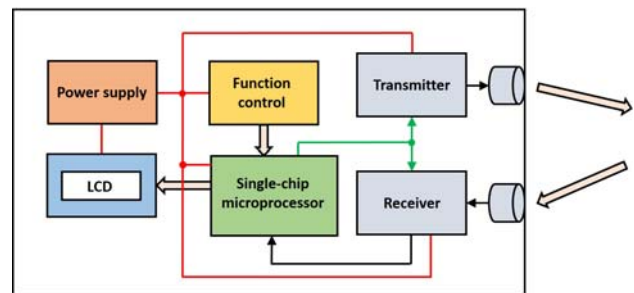


Fig. 1. The block diagram of the module

The piezoelectric ceramic transducer that broadcasts an acoustic wave to space is very important component in the transmitting section. This transducer was soldered from the printed circuit board of the additional module HC-SR04 [14] for the Arduino platform. The additional module HC-SR04 is shown in Fig. 2. The piezoelectric ceramic transducer - transmitter operates at the resonant frequency of 40 kHz.



Fig. 2. The additional module HC-SR04

The detailed block diagram of the transmitting part is shown in Fig. 3. The whole transmitting part works with an asymmetrical supply voltage of +5 and +12 V. As the harmonic signal generator is used here in the Oscillator block Wien bridge [15], based on the operational amplifier TL072 [16]. This generator allows to generate a harmonic signal with frequency in the range of 10 - 100 kHz and also to stabilize the frequency at the desired value. This frequency range is due to the possibility of using another piezoelectric ceramic transducer - transmitter, as well as due to the change of the resonant frequency of the transducer as a function of a temperature. The amplitude of the generated signal is adjustable to the value of 2.5 V. The required settings and value stabilization are controlled by the microcontroller through the Amplitude control and Frequency control blocks based on the digital potentiometers TPL0501 [17]. Subsequently, the signal is amplified by the operational amplifier TL072. This amplifier is set to gain the amplitude of the output signal is 6 V. The Modulator block ensures that the harmonic signal is applied to the piezoelectric ceramic transducer - transmitter with the required number of periods and subsequent disconnection. The selection of the number of periods is again controlled by the microcontroller. The core of the Modulator block is a transistor manufactured with MOSFET technology.

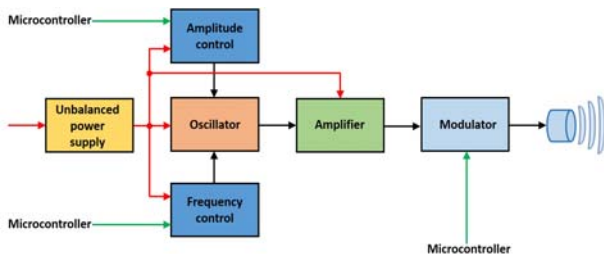


Fig. 3. The detailed block diagram of the transmitter

In the receiving part of the module, the key device is a piezoelectric ceramic transducer that is sensitive to an acoustic wave reflected from an obstacle. This transducer was soldered again from the HC-SR04 addition module and operates again at the resonant frequency of 40 kHz. Detailed scheme of the receiving section is shown in Fig. 4. The whole receiving part works with an asymmetrical supply voltage at the value of +5 V. The signal from the piezoelectric ceramic transducer - receiver enters the Preamplifier block, where it is amplified to the required level for further processing. Operational amplifier TL072 is used here. A Filter block follows to ensure that only the signal with the frequency corresponding to the resonant frequency of the transducer passes through. The basis of this block is an active RC band-pass filter of the fourth order created by two operational amplifiers in the TL072 package. Then the signal enters the Amplifier block, where the final amplification of the signal is performed. This block is again formed by operational amplifier TL072. The signal is then rectified. A one-way rectifier was chosen here using a fast Schottky diode BA159 [18]. To create the received signal envelope, a passive low pass filter is implemented here. Here, the Comparator block serves for the returned acoustic wave detection, which compares the voltage level of the received signal with a constant threshold value or with a value that is set according to the noise level. The choice of these methods is done in the Threshold and Adaptive threshold setting blocks, which a user selects. The signal from the Comparator block is routed to the microcontroller. Here the distance from the obstacle is calculated and the necessary corrections are processed. Distance calculation solves the equation:

$$(1) \quad d = v \cdot t / 2,$$

where: d – distance from an obstacle, v – velocity of an acoustic wave in an open space (air), t – time of an acoustic wave propagation to the obstacle and back (time measured by microcontroller).

The sound velocity of 346.3 ms^{-1} [19] is considered here, which corresponds to the speed of the acoustic wave in dry air at the temperature of 25°C .

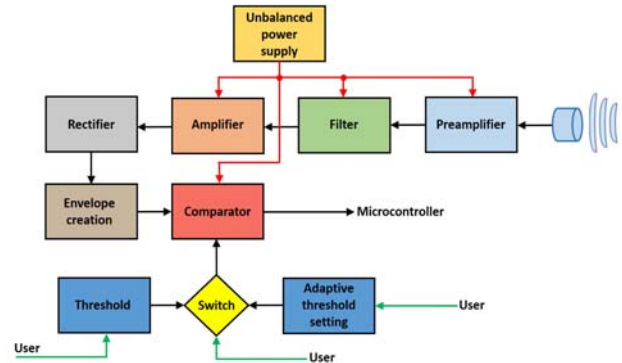


Fig. 4. The detailed block diagram of the receiver

The entire module is made in a compact accomplishment on printed circuit boards significantly using surface mount technology of the components for miniaturization.

The microcontroller algorithm

After the variables and registers declaration and definition, the required frequency, which corresponds to the resonant frequency of the piezoelectric ceramic transducer – transmitter is first checked and alternatively tuned up. The microcontroller then applies a harmonic signal on the specified number of periods to the transducer and starts the time measurement. As soon as it receives a returned reflected acoustic wave signal from the Comparator block, it turns off the time measurement. This time measurement process continues until the selected number of samples is taken to calculate the moving average and thus eliminate inaccurate time measurement. During the measurement, it may happen that the time evaluation is meaningless. The program is equipped with an evaluation algorithm that does not include these values in the moving average. After this process, the distance is calculated. The calculation does not implement a correction for the current barometric pressure, ambient temperature and air humidity, because the designed module does not have the relevant sensors included. The key correction of the calculated distance value is made by a mathematical apparatus using a polynomial correction. The result of the distance measurement is displayed on the LCD. The program also allows entering the menu using the micro buttons and setting the required parameters by a user. After pressing these buttons, the automatic measurement is stopped and the user has the possibility to set the transmission time of the harmonic signal group, the number of periods in the group and the amplitude of the transmitted signal. During each change made, this value is immediately displayed on the LCD. If it is not necessary to set these parameters, it is possible to switch back to automatic mode and the processor works with the initial setting values.

Verification of correct functionality of the module

After the production of printed circuit boards, mounting and cleaning it was necessary to verify the correct functionality and especially the accuracy of measuring the

distance of an obstacle. Testing was performed under laboratory conditions at the temperature of 25 °C. Flat object 50 x 30 cm placed in front of the module was used as an obstacle. First, the range of the proposed module was determined. It has a value of 5 m. A tape meter was used as a reference distance gauge. After determining the range of the designed module, its static characteristic was measured, thus the dependence of the measured distance value on the reference value. The relative error was determined as the precision parameter. The dependence of the relative error of the distance measurement on the reference value is represented in Fig. 5.

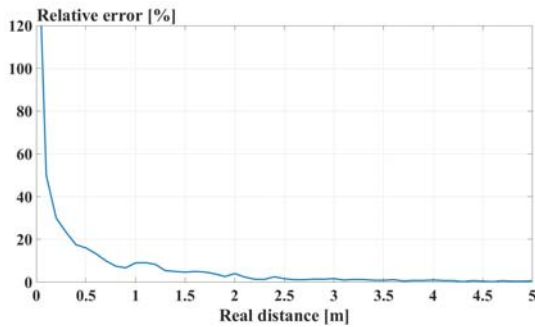


Fig. 5. Dependence of the relative error of the distance measurement on the reference value

The module showed the greatest relative error when the obstacle was in its close proximity. Consequently, the relative error decreased rapidly. At a distance of 0.5 m it was already below 20.0%. Within the distance of 2.0 m, the relative error was decreasing more slowly. At the distance of 2.0 m, it was 4.0%. From the distance of 2.5 m to 5.0 m the module measured the most accurately. Significant statistical characteristics were calculated for accuracy analysis. The maximum relative error was 120.0%, the minimum relative error was 0.2%, and the mean value of relative error was 7.6%.

Subsequently, it was necessary to refine this measurement and apply a correction algorithm. Polynomial correction was used. Thus the aim was to find a correction polynomial. The MATLAB® development environment was used for this operation. The real distance array *Ref* and the measured distance array *Meas* have been defined. Using the *polyfit* function, the array of the polynomial coefficient *PolKoeff* was calculated according to the relation:

$$(2) \quad PolKoeff = polyfit(Meas, Ref, n),$$

where: *n* – is polynomial degree.

The membership of the coefficients from the *PolKoeff* array to the individual members of the polynomial has a decreasing character. The mentioned *polyfit* function uses the mathematical apparatus - least squares method [20]. Three arrays of the correction coefficient for linear, quadratic and cubic polynomials were calculated for the subsequent correction of the measured values. This is presented in the Table 1. Individual polynomials can also be read from this table.

Table 1. Coefficients of the correction polynomials

Meas ³	Meas ²	Meas ¹	Meas ⁰
		1.0128	-0.0812
	9.3713·10 ⁻⁴	1.0080	-0.0771
-0.0030	0.0238	0.9612	-0.0567

These polynomials were then applied to the measured values and an analysis of how relative errors could develop was performed. The dependence of relative errors on the reference value after the application of individual

polynomials together with the original dependence for comparison is represented by Fig. 6.

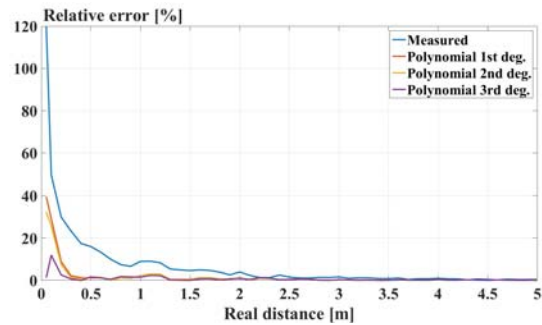


Fig. 6. Dependence of the relative error of the distance measurement on the reference value after the application of individual polynomials with original dependence

In general, it is possible to see that correction polynomials significantly reduce the relative error values compared to the original values. Most significantly, relative errors are suppressed at short distances of the obstacle from the module. With relatively high accuracy it would be possible to measure the distance of 0.3 m when the relative error is already below the level of 1.5%. From the distance value of 1.5 m, the relative error is distinctly below the level of 1.0% in the vast majority of values. From the above depicted image it is also possible to evaluate that the cubic polynomial best suppresses the relative measurement error, especially in the area of the smallest distances of the obstacle from the module. Some statistical indicators were identified as an evidence of the progression analysis of the relative error dependence on the reference value. These statistical indicators included minimum, maximum, and mean relative error values for individual polynomials. These values are represented in Table 2.

Table 2. Statistical indicators of the relative errors progression

Polynomial	Linear	Quadratic	Cubic
Min [%]	0.0060	0.0024	0.0057
Max [%]	39.5861	32.3774	11.9783
Mean [%]	2.1347	1.8825	0.8287

After this evaluation, the cubic polynomial was implemented to the single-chip microprocessor of the designed module. The applied correction algorithm has the following form:

$$(3) \quad DistCor = -0.0030 \cdot Meas^3 + 0.0238 \cdot Meas^2 + 0.9612 \cdot Meas - 0.0567,$$

where: *DistCor* – is corrected distance, *Meas* – is measured value of distance.

After programming of this correction algorithm into the single-chip microprocessor of the module, the static characteristic was again measured and the relative error analysis was performed. The dependence of the relative error of the distance measurement on the reference value is shown in Fig. 7.

Again, the original curve in blue is depicted here, further, the expected progress of relative errors in red, and real measured dependence of the relative error on the reference value in yellow, are shown. As it is possible to see in the graph, implementation of the correction algorithm into the microprocessor, the module shows even better values after the overall evaluation than the simulation performed. This is best seen in the smallest distances of the obstacle from the module, even below the distance of 0.3 m. A significantly worse area of the measurement accuracy was in the range of 0.5 - 0.7 m. Statistical indicators were again evaluated as

a proof of the correct measurement of the module distance. The minimum value of the relative error was 0.0%, the maximum relative error was 4.1%, and mean relative error was 0.6%.

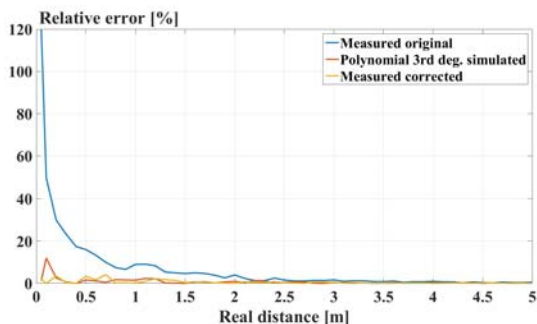


Fig. 7. Dependence of the relative error of the distance measurement on the reference value after applying the correction algorithm to the module

Conclusion

The paper presented complete design of the distance measurement module using piezoelectric ceramic transducers commonly available at the market. An important part of the article was thorough description of the transmitting and receiving part of the module. The individual parts have their specifics. The module allows controlling the amplitude and frequency of the transmitted signal. It allows generating a harmonic signal for the future possibility of a phase modulation. It is also equipped with a device for automatic signal amplification and setting a threshold for signal detection. The entire module is made in a compact design on printed circuit boards with surface mount technology to miniaturize the entire device.

Relative errors analysis was chosen to verify the correct function of the module. The initial dependence of the relative error of distance measurement on the reference value was measured. As a correction algorithm, the application of polynomial was selected. Simulation of relative errors progression was performed using three correction polynomials. According to the simulation the best properties reached the cubic polynomial. It significantly reduced relative error values even at small distances of the obstacle from the module. After implementing of this correction polynomial into the module microcontroller, the algorithm showed even better properties than simulations.

The aim of possible further work on the issue is to increase the range of the module while maintaining the achieved accuracy. This would be possible to achieve by implementing signal modulation, especially phase modulation, even at the cost of greater signal generator complexity. The distance measurement is also possible to be refined with this method.

The work presented in this article has been supported by the Czech Republic Ministry of Defence – University of Defence development program “Research of sensor and control systems to achieve battlefield information superiority”.

Authors: Ing. Přemysl Janů, Ph.D., University of Defence in Brno, Department of Communication Technologies, Electronic Warfare and Radiolocation, Kounicova 65, 662 10, Brno, E-mail: premysl.janu@unob.cz; Ing. Radim Šrámek, University of Defence in Brno, Department of Communication Technologies, Electronic Warfare and Radiolocation, Kounicova 65, 662 10, Brno, E-mail: radim.sramek3@unob.cz.

REFERENCES

- [1] Bereziuk O., Lemeshev M., Bogachuk V., Wójcik W., Nursetova K., Bugubayeva A., Ultrasonic Microcontroller Device for Distance Measuring Between Dustcart and Container of Municipal Solid Wastes, *Przegład Elektrotechniczny*, 1 (2019), nr 4, 148-152
- [2] Krishnan P., Design of Collision Detection System for Smart Car Using Li-Fi and Ultrasonic Sensor, *IEEE Transactions on Vehicular Technology*, 67 (2018), nr 12, 11420-11425
- [3] Jestop Jeswin C., Marimuthu B., Chithra K., Ultrasonic Water Level Indicator and Controller Using AVR Microcontroller, *International Conference on Information, Communication & Embedded Systems (ICICES 2017)*, 2017, 1-6
- [4] Shaoyong Z., Research of Ultrasonic Distance Measurement Device, *6th International Conference on Wireless Communications Networking and Mobile Computing (WiCOM)*, 2010, 1-3
- [5] Biqiang D., Shizhao L., A Common Obstacle Avoidance Module Based on Fuzzy Algorithm for Unmanned Aerial Vehicle, *The 6th Annual IEEE International Conference on Cyber Technology in Automation, Control and Intelligent Systems*, 2016, 245-248
- [6] Jingjing D., Shuiying Z., Xuebo J., Guohong Y., The Design of Ultrasonic Distance Measurement System Based of SOPC, *Third International Conference on Intelligent Human-Machine Systems and Cybernetics*, 2011, 166-168
- [7] Dycka P., Janu P., Dub M., Bajer J., Bystricky R., Influence of Extreme Temperature on Characteristics of Electric Equivalent of Piezoceramic Transducer, *7th International Conference on Military Technologies, ICMT 2019*, 2019, 1-5
- [8] MCUST16A40S12RO, 2019, available from: https://cz.farnell.com/multicomp/mcust16a40s12ro/transmitter-40khz-16mm-metal/dp/2362669?ost=MCUST16A40S12RO&ddkey=https%3Acz-CZ%2FElement14_Czech_Republic%2Fsearch
- [9] MCUSR16A39S12RO, 2019, available from: https://cz.farnell.com/multicomp/mcusr16a39s12ro/receiver-39khz-16mm-metal/dp/2362670?ost=MCUSR16A39S12RO&ddkey=https%3Acz-CZ%2FElement14_Czech_Republic%2Fsearch
- [10] IIC I2C Display, 2020, available from: <https://arduino-shop.eu/arduino-platform/1570-iic-i2c-display-lcd-1602-16x2-characters-lcd-module-blue.html>
- [11] L78M05ACDT-TR, 2019, available from: <https://cz.farnell.com/stmicroelectronics/l78m05acdt-tr/linear-voltreg-reg-5v-0-5a-to/dp/2463950?st=L78M05>
- [12] TS78M12CP ROG, 2019, available from: <https://cz.farnell.com/taiwan-semiconductor/ts78m12cp-rog/linear-volt-reg-12v-500ma-to-252/dp/2747641?st=78M12>
- [13] The Original Development Kit Arduino Nano, 2020, available from: <https://arduino-shop.eu/arduino-platform/1474-the-original-development-kit-arduino-nano.html>
- [14] Arduino Distance Meter Ultrasonic, 2020, available from: <https://arduino-shop.eu/arduino-platform/846-arduino-distance-meter-ultrasonic.html>
- [15] The Wien Bridge Oscillator, 2019, available from: https://www.electronics-tutorials.ws/oscillator/wien_bridge.html
- [16] TL072ACD, 2019, available from: <https://cz.farnell.com/texas-instruments/tl072acd/ic-op-amp-dual-jfet-smd-soic8/dp/3117782?st=TL072>
- [17] TPL0501-100DCNR, 2019, available from: <https://cz.farnell.com/texas-instruments/tpl0501-100dcnr/dgtl-pot-256pos-100k-sot23-8/dp/3124098?st=TPL0501>
- [18] BA159+, 2019, available from: <https://cz.farnell.com/multicomp-pro/ba159/rectifier-single-1kv-1a-do-204al/dp/2675054?st=BA159>
- [19] Ultrasound, 2020, available from: <https://courses.washington.edu/bioen508/Lecture6-US.pdf>
- [20] Polyfit, 2020, available from: https://ch.mathworks.com/help/matlab/ref/polyfit.html?s_tid=srchtml